Mechanical behavior of mycelium-based particulate composites

M. R. Islam, G. Tudryn, R. Bucinell, L. Schadler & R. C. Picu

Journal of Materials Science
Full Set - Includes `Journal of Materials Science Letters'

ISSN 0022-2461

J Mater Sci
DOI 10.1007/s10853-018-2797-z

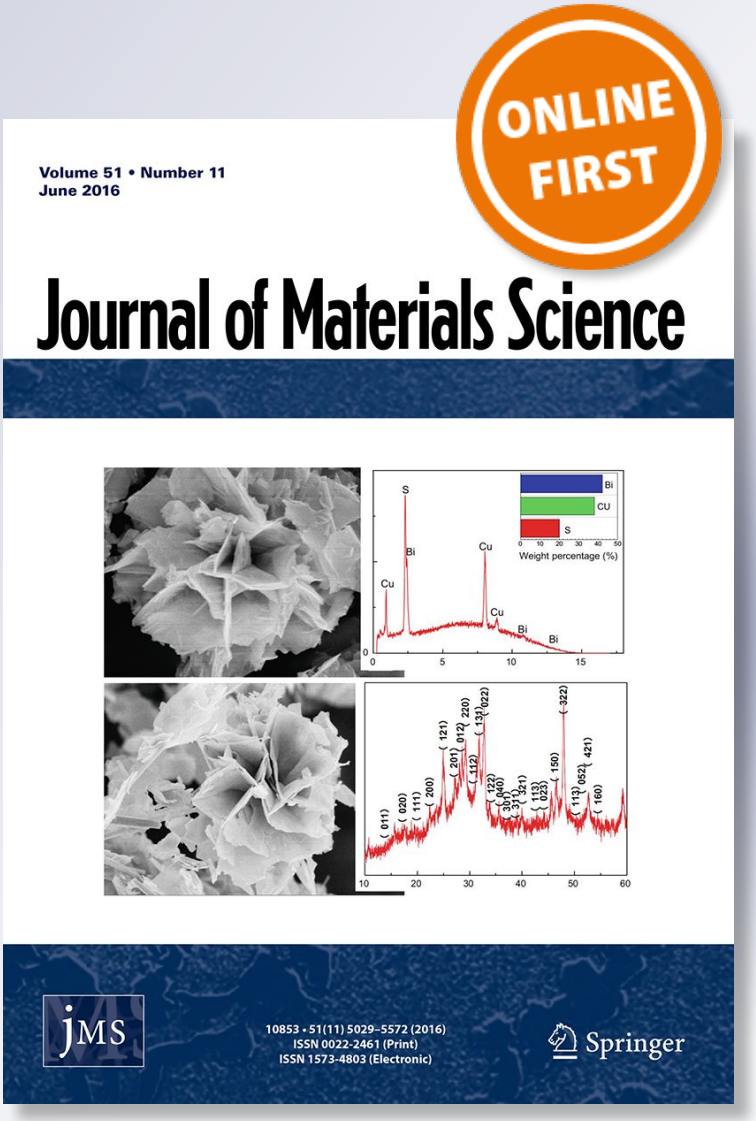

Springer

J Mater Sci

Composites

Mechanical behavior of mycelium-based particulate composites

M. R. Islam[1], G. Tudryn[2], R. Bucinell[3], L. Schadler[4], and R. C. Picu[1,*]

[1] Department of Mechanical, Aerospace and Nuclear Engineering, Rensselaer Polytechnic Institute, Troy, NY 12180, USA
[2] Ecovative Design LLC, Green Island, NY 12183, USA
[3] Department of Mechanical Engineering, Union College, Schenectady, NY 12308, USA
[4] Department of Material Science and Engineering, Rensselaer Polytechnic Institute, Troy, NY 12180, USA

Received: 25 May 2018
Accepted: 10 August 2018

ABSTRACT

This work investigates the mechanical behavior of mycelium composites reinforced with biodegradable agro-waste particles. In the composite, the mycelium acts as a supportive matrix which binds reinforcing particles within its filamentous network structure. The compressive behavior of mycelium composites is investigated using an integrated experimental and computational approach. The experimental results indicate that the composite mimics the soft elastic response of pure mycelium at small strains and demonstrates marked stiffening at larger strains due to the densification of stiff particles. The composite also exhibits the characteristic stress softening effect and hysteresis under cyclic compression previously observed for pure mycelium. To gain further insight into the composite behavior, a three-dimensional finite element model based on numerical homogenization technique is presented. Model validation is performed by direct comparison with experiments, and a parametric study of the effect of mycelium density and particle size is discussed.

Introduction

Many natural materials have fibrous architecture. Examples are numerous, including silk spider webs [1], bone [2], plant stems such as bamboo [3], connective tissue [4]. The design of these natural materials has inspired researchers to mimic such architectures in synthetic materials, although this proves to be a challenging task in many cases [5]. A novel approach to this problem is to construct engineering components by directly growing the natural material into the desired shape. Such components inherit the microstructure and properties of the base material. With this motivation, we study here a unique composite material composed from a mycelium matrix embedding stiffer, biodegradable reinforcing particles.

Mycelium is the vegetative part of fungi and is composed from tube-like fibers of diameter of approximately 1 μm, called hypha. Hypha grow by apical tip elongation and occasionally branch out or merge with other hyphae, forming a random fiber

Address correspondence to E-mail: picuc@rpi.edu

https://doi.org/10.1007/s10853-018-2797-z

Published online: 16 August 2018

network-like structure [6]. The wall of a hypha consists of chitin nanofibrils which provide its stiffness and strength [7]. Biologically active hyphae bind to and/or digest organic material by applying mechanical forces and secreting hydrolytic enzymes [8]. Consequently, a natural composite system results in which mycelium functions as a supporting matrix embedding particles that function simultaneously as nutrition and reinforcement. In this paper, we focus on mycelium composite with agro-waste particles as reinforcements, as shown in Fig. 1.

The mycelium composite is inherently a multiscale material where reinforcing particles are on the order of 1–5 mm (Fig. 1c), and fiber segments of the mycelium network are on the order of few microns in length (Fig. 1d). The matrix phase of the composite is a random fiber network (Fig. 1d), and hence bonding is discontinuous at the particle–matrix interface. To facilitate the discussion, we briefly review the key characteristics of pure mycelium network here, based on our recent work [9].

In uniaxial tension, unfilled mycelium exhibits a linear elastic regime up to $\sim$ 8% strain, followed by a linear strain hardening regime before rupture at a strain of $\sim$ 25–30%. The elastic modulus varies as a quadratic function of density, and the strength is proportional to the network density to power 3/2. Under compression, mycelium exhibits an elastic regime at small strains, followed by a strain localization regime in which the effective tangent stiffness decreases considerably due to the elastic–plastic buckling of fibers. A densification regime is observed at larger strains, in which the large number of fiber-to-fiber contacts forming under global compression induces rapid stiffening. A similar behavior is observed during the compression of open cell foams [10] and soft materials like fibrin networks [11]. During the strain localization regime, the deformation proceeds through the formation of multiple bands of localized strain that connect the weakest domains in the material. Under cyclic compression mycelium also exhibits significant hysteresis and the stress softening behavior known as the Mullins effect—a feature it shares with filled and unfilled elastomers [12, 13].

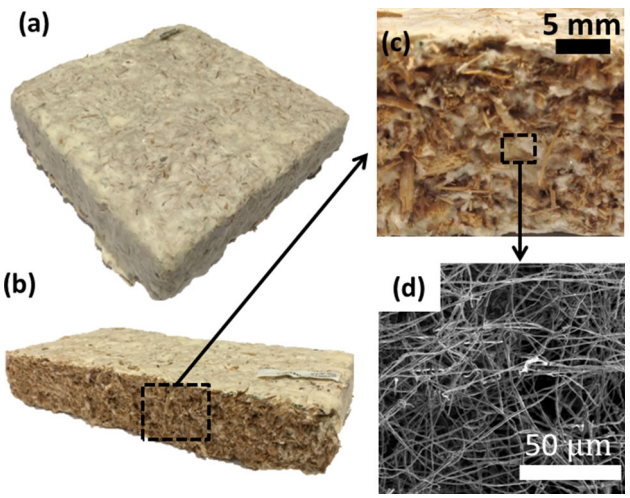

Figure 1 Mycelium composite at various scales: **a** macroscale sample (6″ × 6″ × 1″), **b** cross section of the macroscale sample (6″ × 1″), **c** zoomed view (5 mm scale bar) of the cross section showing particle (brown) distribution within mycelium matrix (white), and **d** SEM micrograph of mycelium microstructure (50-μm scale bar).

Previous work on mechanical characterization of mycelium composites is scarce in the literature. Holt et al. [14] studied mycelium composites with cotton plant biomass (CPB) as reinforcement, aiming to evaluate the effect of six blends of CPB on the composite properties. They developed composites with density ranging from 66 to 224 kg/m^3 and observed that the elastic modulus of the composite varies in the range 120 to 670 kPa. Travaglini et al. [15] reported higher elastic modulus of 1.3 MPa and compressive yield strength of 47.5 kPa for a woodchip-mycelium composite with density of 318 kg/m^3. Zhang et al. [16] studied the influence of packing condition, incubation time and mycelium deactivation on composite properties for various substrate materials. While these studies provide useful properties of several mycelium composites, a systematic and detailed understanding of the mechanical behavior of mycelium composite is yet to be established.

The mycelium composite considered in this work is a naturally grown engineered material with several advantages over fibrous or cellular artificial materials, such as low density, low energy consumption during production, and biodegradability. It is obtained by seeding mycelium on organic material (corn stover). The mycelium grows on and consumes some of the organic particles, embedding them in the hyphae network at the same time. The process is stopped by thermal treatment at the desired mycelium density. Such material has the potential to replace petroleum-based polymeric materials used today in a variety of applications, such as in packaging, while being environmentally benign.

However, at this stage, the relationship between process parameters and the material structure is poorly understood, while its mechanical properties have not been explored. This report presents the groundbreaking work in this direction. We observe that this material has nonlinear mechanical behavior, largely dictated by the mycelium matrix, including strain-dependent hysteresis and stress softening under cyclic loading. The mechanical properties are independent of the filler particle size and aspect ratio, in the range of parameters considered. Based on these experimental observations, a two-scale finite element model is developed which captures the mechanics at the mycelium network scale, as well as the overall behavior of the composite on the macroscale. The model is calibrated based on a set of experimental data and subsequently validated by comparison with additional experimental results. The model is then used to predict material behavior for inclusions of different aspect ratio and dimensions, i.e. in a material parameter space in which experiments were not performed. The model can be further used to advance this type of materials while reducing the amount of experimentation required.

Materials and methods

Sample preparation

Ecovative Design, LLC, manufactured the test specimens. The composite samples were prepared similar to the pure mycelium samples, as described in [9]. Here the mycelium vegetative tissue is first inoculated in a filter patch bag in the presence of corn stover particles and with nutrition (calcium and carbohydrate) and water. Mycelium is allowed to grow at room temperature ($\sim$ 25 °C) for 4 days, and then it is ground into small pieces in order to redistribute the growth evenly. Next, the material is packed into rectangular molds (6″ × 6″ × 1″) and allowed to grow further for four additional days. As a last step, the samples are heat-treated at 100 °C for four hours to render the material biologically inactive and stop hyphae growth.

Morphological characterization

The mass density of the composites, m_c/V_c, is measured using the density ASTM standard C303. The amount of biomass (m_m) per unit mass of the composite is measured using high-performance liquid chromatography (HPLC) with ergosterol (sigma, 98%) standards for relative quantification of dry mass. The volume fractions of reinforcement particles, ϕ_f, and mycelium, ϕ_m, phases are calculated using Eqs. (1) and (2). Note that the particle volume fraction changes slightly as the composite grows since the mycelium consumes part of the corn stover as it grows. This emphasizes the need to evaluate these measures after the growth is stopped.

$$\phi_f = \frac{(m_c - m_m)/\rho_{corn}}{V_c} \tag{1}$$

$$\phi_m = 1 - \phi_f \tag{2}$$

Mechanical testing

Uniaxial compression tests were conducted using an EnduraTec Elf 3200 mechanical testing machine (BOSE, Eden Prairie, MN) under displacement control, and all the tests were performed in ambient conditions (25 °C and $\sim$ 50% relative humidity). Cuboid specimens of dimensions 20 mm × 20 mm × 16 mm were used for compression testing. The specimens were deformed at a rate of 6.25×10^{-3} s^{-1} up to stretches ranging from 0.8 to 0.95. Cyclic loading tests under both constant and increasing strain levels in each cycle have been performed under compression. No hold/relaxation was applied between cycles.

Experimental

Morphology

Four different reinforcing particle size ranges are used in different samples in order to study the filler size effect on macroscopic properties. We define these as "small" fillers, of sizes ranging from 0.4 to 0.9 mm, "medium" fillers, of sizes ranging from 0.9 to 1.7 mm, and "large" fillers, of size in the range 1.7–6.7 mm. Here, "size" refers to the largest dimension of individual fillers. Samples in which fillers can have any dimension in the broad range 0.4–6.7 mm are also considered and are labeled "all". Figure 2a, b shows

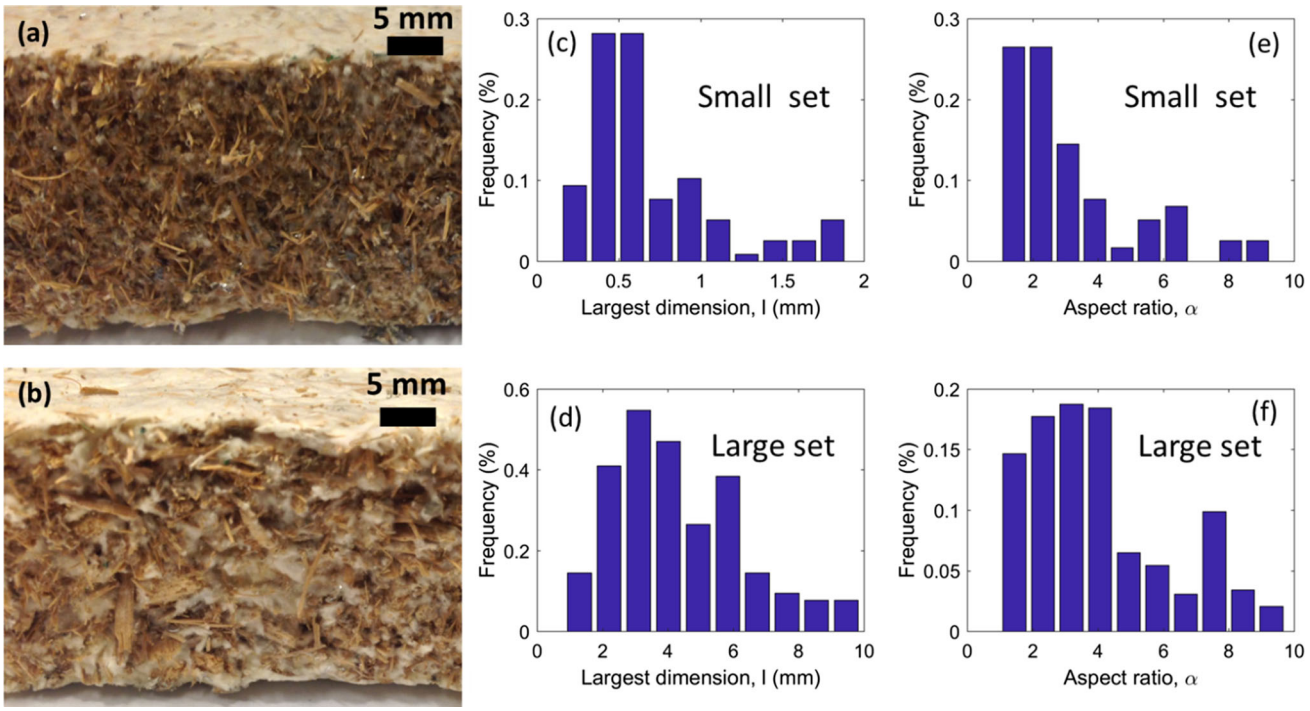

Figure 2 Cross sections of composite with **a** "small" and **b** "large" particles. Distributions of the largest dimension (l) and aspect ratio (α) for "small" and "large" particles are shown in **c**–**f**.

images of cross sections of composites with "small" and "large" particles, respectively. The distribution of the longest and shortest dimensions of particles is determined by microscopy for each set. Figure 2c, d shows the distribution of the largest particle dimension (l) for samples from the "small" and "large" particle size categories, respectively. Figure 2e, f shows the distribution of the aspect ratio for samples from the same two categories. The distributions are rather broad in all cases. The mean aspect ratio of the "small" particles is on the order of 3, while that of the "large" particles is close to 5.

Table 1 shows the total mass density of the composite, ρ_c, the density of mycelium, ρ_m, and the volume fractions of mycelium and reinforcing particles for the four particle sizes considered. For each particle size set, four specimens are characterized and the means are shown in Table 1. It is observed that the volume fractions of mycelium ($\phi_m \sim 0.7$) and reinforcement phases ($\phi_f \sim 0.3$) are approximately the same for all these composites.

Generic compressive response of composites

Figure 3a shows the generic stress–strain response of mycelium composites under uniaxial compression. The stress and strain measures used here are the nominal stress, or the first Piola–Kirchhoff stress (S), and the stretch (λ). It is observed that the composite response is soft and stress varies approximately

Table 1 Morphological properties of mycelium composites with various particle sizes. The range of variation of the composite density is approximately 10% of the mean in all cases

Particle size set	Composite density $\rho_c \left(\mathrm{kg/m^3}\right)$	Mycelium density $\rho_m \left(\mathrm{kg/m^3}\right)$	Mycelium volume fraction (ϕ_m)	Corn filler volume fraction (ϕ_f)
Small (0.4–0.9 mm)	121.6 ± 5.41	10.34 ± 0.46	0.722 ± 0.012	0.28
Medium (0.7–1.7 mm)	121.0 ± 6.97	10.92 ± 0.59	0.706 ± 0.016	0.28
Large (1.7–6.7 mm)	133.0 ± 1.29	11.30 ± 0.11	0.695 ± 0.003	0.31
All (0.4–6.7 mm)	128.4 ± 6.94	10.28 ± 0.61	0.723 ± 0.015	0.30

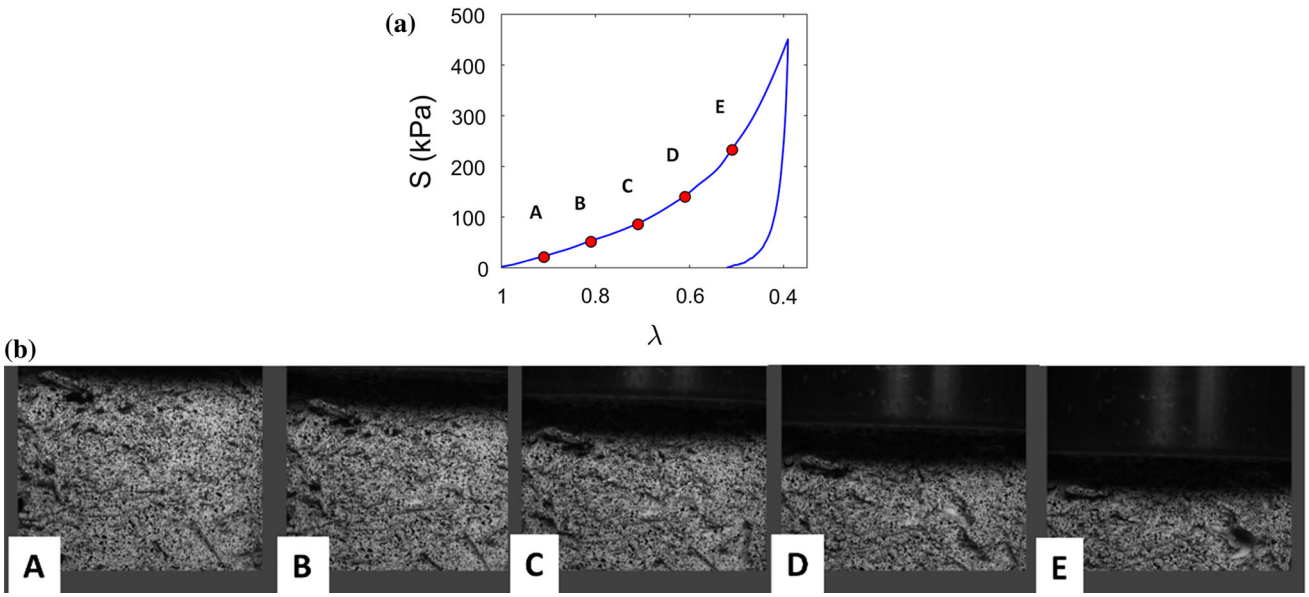

Figure 3 **a** Generic stress–strain response of mycelium composite under compression and **b** deformed configurations for various strain levels (corresponding to points (A–E) in **a**.

linearly with the stretch for $1 > \lambda \geq 0.8$. In this regime, the behavior is largely controlled by the soft mycelium matrix and load transfer is limited due to discontinuous bonding between matrix and fillers. For $\lambda \leq 0.8$, a gradual stiffening response is observed, indicating an increase in the contribution of fillers as the material is compacted. Rapid stiffening is observed for large compactions ($\lambda \leq 0.6$).

Deformed configurations of the sample at various stretches (corresponding to points (A) to (E) in Fig. 3a) are shown in Fig. 3b. It is observed that deformation in the composite is relatively uniform and does not exhibit localization bands, which is different from observations in unfilled mycelium [9]. In pure mycelium, the deformation localizes in multiple bands that form at the lower density sub-domains of the material. In the composite, the stiffer reinforcement particles diminish strain localization and prohibit the collapse of the surrounding mycelium network.

Effect of particle size

Figure 4a shows the stress–strain curves for composites with different particle sizes (Table 1). The curves represent the average of four test specimens, and the bars indicate the range of the four specimens. The generic trend of the stress–strain curves is not sensitive to the particle size. Furthermore, the modulus of elasticity measured from loading (E_c) and unloading (E_c^u) branches of the stress–strain curves is also not affected significantly by the particle size, as illustrated in Fig. 4b, c. Specifically, E_c ranges from 0.14 to 0.19 MPa, and E_c^u ranges from 1.6 to 2.7 MPa. This is expected if the behavior of the composite under small strains is controlled primarily by that of the mycelium matrix.

Cyclic loading behavior

The response of mycelium composites to cyclic loading is also investigated. Samples with "large" particles were considered in this study. Figure 5a shows the cyclic stress–strain response for three successive cycles with increasing strain amplitude in each cycle. No hold time or relaxation is imposed between cycles. Unloading is performed immediately after loading with the same strain rate ($6.25 \times 10^{-3}\,s^{-1}$). Interestingly, the composite exhibits similar cyclic stress softening and hysteresis as reported previously for pure mycelium [9]. This indicates that, although the filler volume fraction is large, the matrix controls the response in compression at stretches $1 > \lambda \geq 0.8$ (or below 20% engineering stress).

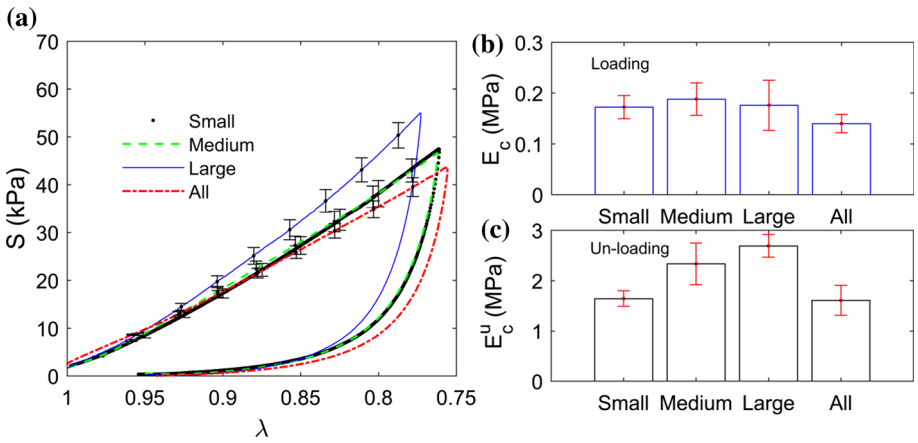

Figure 4 Effect of particle size on mechanical properties of mycelium composites: **a** stress–stretch curves, and **b** the dependence of the loading modulus (E_c) and **c** unloading modulus (E_c^u) on filler size. The error bars represent the range of four test samples.

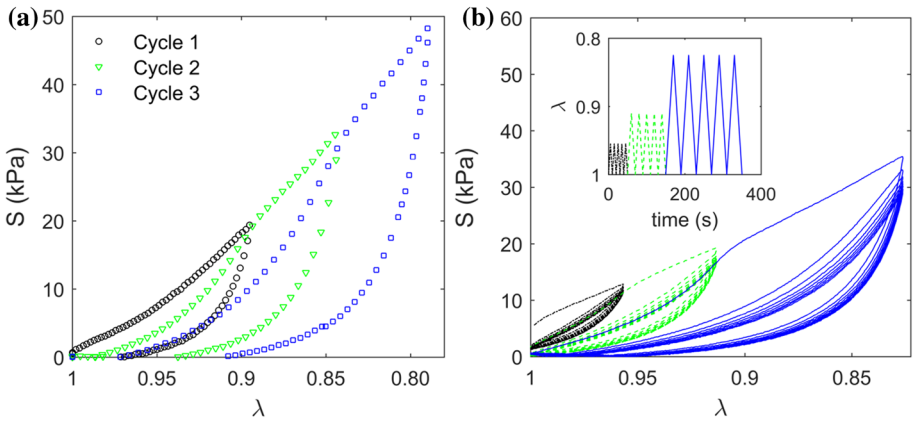

Figure 5 Stress–strain response of mycelium composites with "large" fillers under cyclic compression: **a** successive cycles with increasing strain amplitude, and **b** response to a loading sequence with three periods of increasing strain amplitude, each being composed from five successive cycles of constant strain amplitude (see inset).

Subsequent cycles produce a stress smaller than in the first cycle at strains smaller than those reached in the previous cycles. If the strain becomes larger than that experienced previously, the curve converges to the monotonic loading curve. This behavior is similar to the Mullins effect observed in filled and unfilled rubbers [13]. The detailed mechanisms leading to the Mullins effect are not entirely understood, but it is generally accepted that this behavior is due to the accumulation of internal damage. In mycelium, fiber damage and rearrangement may lead to the observed softening.

If multiple cycles are performed with the same maximum strain, softening is substantial in the first cycle, after which the cyclic response stabilizes to a curve that exhibits hysteresis (Fig. 5b). When the imposed strain exceeds the strain level of the previous cycles, the loading curve gradually converges to the primary loading path, just as seen in Fig. 5a for single cycles of increasing amplitude. The size of the hysteresis loop, and hence the energy dissipated per cycle, increases with increasing maximum applied load.

Modeling of mycelium composite

A model able to predict the mechanical behavior of mycelium composite with specific microstructure is desirable in the effort to further develop this type of materials. Such model can be used to explore the material parameter space beyond the range easily accessible experimentally and hence can be used as an effective material design tool. We present such a model in this section.

Mycelium composites are multiscale materials with at least two essential scales: the scale of the reinforcement particles (mesoscale) and that of the

mycelium network (microscale). With particles ranging in size from hundreds of microns to mm, and mycelium with fiber diameter on the order of 1 μm and inter-fiber pores on the order of tens of microns, a clear scale separation exists between the micro- and mesolevels. However, the matrix may exhibit density fluctuations on scales intermediate between the micro- and mesoscales, which leads to substantial modeling complexities.

Here we adopt a two-scale numerical homogenization approach based on finite elements representation, as shown schematically in Fig. 6. In numerical homogenization, the notion of representative volume element (RVE) plays the pivotal role in determining the effective properties of the random material. The RVE is the smallest volume whose predictions provide representative estimate of the composite behavior [17]. The RVE should contain sufficient number of inclusions in order to be statistically representative [17, 18]. Here, a 3D cubic RVE model is developed to represent the macroscale of the composite, where the discrete mycelium matrix is represented as a homogenized continuum phase and reinforcement particles are represented as randomly distributed cylindrical inclusions. The constitutive behavior of the mycelium phase is derived from the multiscale stochastic continuum model (shown in the dashed box of Fig. 6), developed for pure mycelium in our previous work [9, 19]. The reinforcement particles are modeled as linear elastic with modulus (E_f) 1.5 MPa and Poisson ratio (ν_f) 0.3 as per manufacturers specifications for corn stover [20].

The stochastic continuum model of pure mycelium (the composite matrix) combines a microscale random fiber network (RFN) model and a macroscale continuum model. The microscale model captures network scale behavior, explicitly taking into account

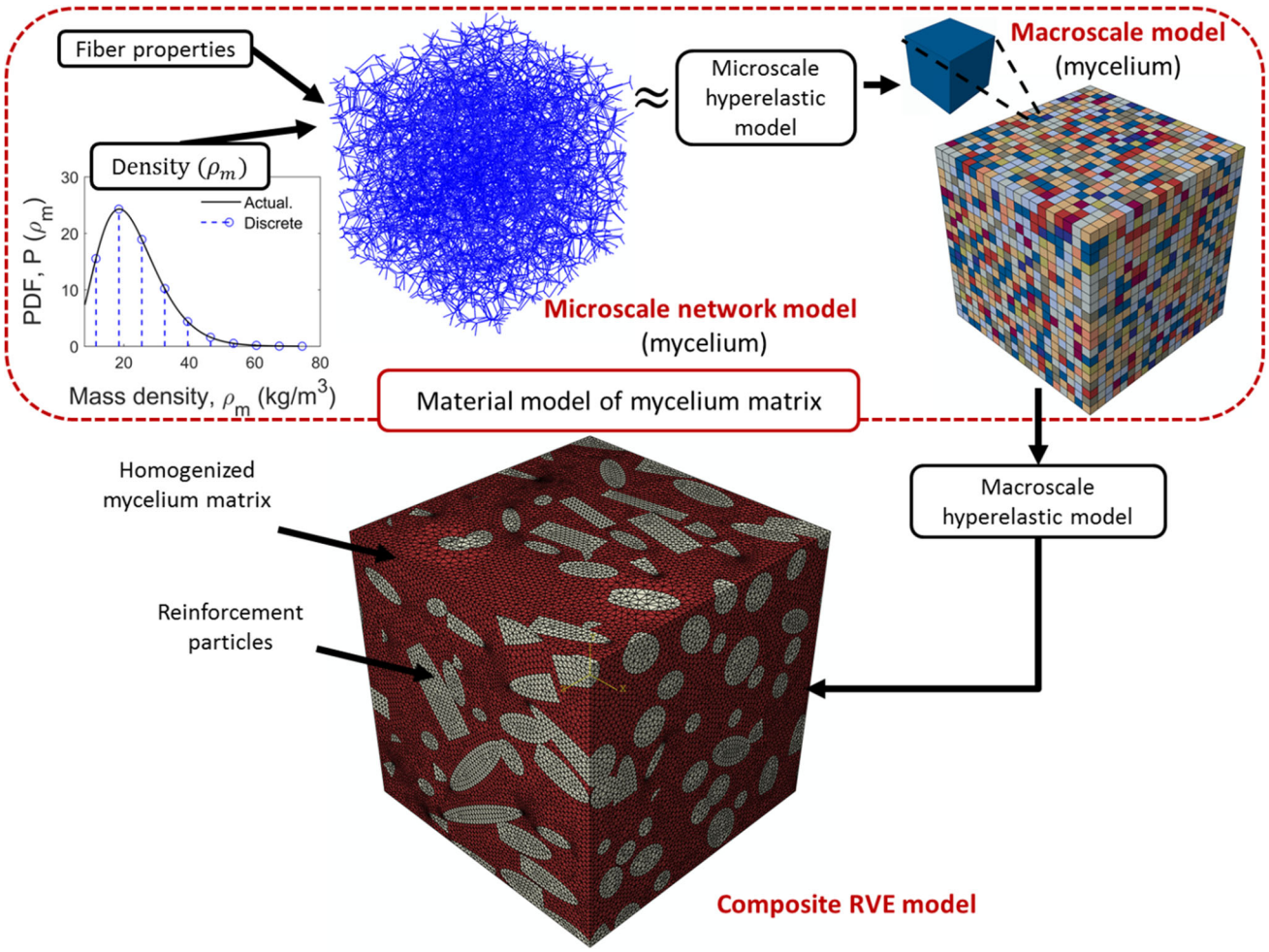

Figure 6 Schematic representation of the multiscale modeling procedure developed for mycelium composites.

hyphal (mycelium fiber) properties and density. The macroscale continuum model consists of sub-domains of variable density representing mesoscale density fluctuations on a length scale much larger than the microscale. The density of a sub-domain is sampled from an experimentally calibrated distribution, and the constitutive equation of the sub-domain is defined by the RFN model with the respective sampled density. Specifically, the computed stress–strain response of the RFN model is fitted with a hyperelastic constitutive equation (shown as microscale hyperelastic model in Fig. 6) which is then used in the macroscale continuum model. The macroscale continuum model of pure mycelium is simulated under prescribed loading, and the resultant stress–strain response is fitted to another hyperelastic constitutive equation (shown as mesoscale hyperelastic model in Fig. 6), which is further used to represent the matrix phase in the macroscale composite RVE model. In the following sub-sections, these modeling steps are discussed in detail.

Composite RVE generation

To generate the RVE model with high volume fraction of reinforcement particles ($\phi_f \approx 0.3$), we use the fiber packing method presented in [21]. The method combines the random sequential adsorption (RSA) algorithm [22] and a dynamic FEM simulation. In the first step, RSA is used to generate non-overlapping particle assemblies of relatively low density in six pseudo-composite boxes. The particles are idealized as cylinders of length (l) and aspect ratio (α). The particle dimensions (l, α) are sampled from the experimental distributions of Fig. 2. We consider only the "large" particle set here. In the second step, the six particle assemblies are packed into the target model box by a direct dynamic FEM simulation of the packing process. In this finite element model, particles are discretized as beam elements and surface-to-surface contacts are allowed to occur in order to prevent inclusion overlap during packing. These simulations were performed using the commercial solver Abaqus/Explicit (version 6.13-1) [23]. In the current work, the RVE size is selected to be three times the largest particle size (l) to reduce model size effects [24].

The generated composite RVEs (Fig. 6) are meshed using Simmetrix Inc. meshing tools, MeshSim [25]. We use a relative mesh size of 0.1 (approximately 10 elements along the largest dimension) to ensure reasonable mesh quality throughout the model. Additionally, we consider curvature-based mesh refinement with relative size 0.05 to obtain a finer mesh at the particle–matrix interface. We use linear 3D tetrahedral elements to reduce computational cost. A typical model contains approximately 5×10^5 elements. To account for the stochasticity of particle packing, we consider three replicas of the RVE model in each case. The uniaxial compression of the RVE model is performed in displacement control using Abaqus/Standard as finite element solver.

Material model of mycelium matrix

Microscale network model

A Voronoi network, constructed by partitioning the domain into convex polygons and placing fibers along the edges of polygons, is used as the microscale model of pure mycelium. The material density (ρ_m) is assumed constant at this scale and uniquely defined as $\rho_m = \left(1/L_N^3\right)\rho_h A_h L_h$ where L_N is the size of the cubic domain, ρ_h is the density of hypha (mycelium fiber) material, A_h is the cross-sectional area of a typical tubular hypha, and the L_h is the total hypha length in the domain. Hyphae are assumed to have the same outer diameter (d_0 = 1.3 μm, measured from SEM images) and wall thickness (t_w = 100 nm [26]). An elastic–plastic material model based on chitin properties (Young's modulus $E_h = 2.5\,\text{GPa}$, yield stress $\sigma_h = 45\,\text{MPa}$, Poisson ration $\nu_h = 0.3$, and density $\rho_f = 1430\,\text{kg/m}^3$) [27] is used for hyphae. Beyond the elastic regime, the material behavior is assumed to be linear with a strain hardening slope of 2% of E_h (bilinear elastic–plastic model). Networks of ten densities in the range 8–80 kg/m^3 are simulated under uniaxial compression, and their mechanical response is fitted with the microscale hyperelastic model.

Microscale hyperelastic model

The microscale hyperelastic model is based on a strain energy density function of Ogden type [28]:

$$U = U(\mathbf{C}) = W(\lambda_1, \lambda_2, \lambda_3) = \sum_{i=1}^{N} \frac{2\mu_i}{\alpha_i^2}\left(\lambda_1^{\alpha_i} + \lambda_2^{\alpha_i} + \lambda_2^{\alpha_i} - 3 + \frac{1}{\beta_i}\left(J^{-\alpha_i\beta_i} - 1\right)\right) \quad (3)$$

where μ_i, α_i and β_i are material coefficients and $\lambda_j (j = 1, 2, 3)$ are principal stretches. J is the determinant of the deformation gradient ($J = \lambda_1\lambda_2\lambda_3$), and N is the number of terms in the series. Under uniaxial loading, the nominal stress in the loading direction, S_L, is computed as:

$$S_L = \frac{\partial U}{\partial \lambda_L} = \frac{2}{\lambda_L}\sum_{i=1}^{N} \frac{\mu_i}{\alpha_i}\left(\lambda_L^{\alpha_i} - J^{\alpha_i\beta_i}\right). \quad (4)$$

Coefficients (μ_i, α_i and β_i) are determined by fitting the computed mechanical response of the microscale network model. We use $N = 3$ and the hyperelastic formulation discussed here is implemented through the HYPERFOAM material model available in Abaqus. Details of the hyperelastic coefficients for various network densities are provided in our previous work [19]. The microscale hyperelastic model is used as constitutive input for the macroscale continuum model of pure mycelium.

Macroscale continuum model

The macroscale model representing pure mycelium is a cubic RVE continuum composed from 8000 sub-domains, with the mycelium density varying from one sub-domain to another in an uncorrelated manner. The material density (ρ_m) of sub-domains is assumed to follow a beta distribution defined as:

$$P(\rho_m|\alpha, \beta) = \frac{\rho_m^{\alpha-1}(1-\rho_m)^{\beta-1}}{B(\alpha, \beta)}, \quad (5)$$

where B is the Beta function, $B(\alpha, \beta) = \Gamma(\alpha)\Gamma(\beta)/\Gamma(\alpha+\beta)$, Γ is the Gamma function, and (α, β) are shape parameters. The mean (μ) and variance (σ^2) of the mycelium density distribution are calibrated (see, ref [9] for details) by comparing the strain distribution in the model with the strain distribution of pure mycelium samples measured by digital image correlation (DIC). An iterative search method is used for this purpose. The resulting values of these parameters are ($\mu = \rho_m$, $\sigma/\mu = 0.48$). Here, we focused on modeling the response of composites with a "large" particle set and hence the mean mycelium density used is $\rho_m = 11.3\,\mathrm{kg/m^3}$, Table 1. Further, the distribution of Eq. (5) is approximated by a set of delta functions equally spaced in the range 8–80 $\mathrm{kg/m^3}$. The mechanical behavior of microscale models representing networks with each of these densities is computed and fitted with the microscale hyperelastic model, which is then used as constitutive input for sub-domains of the macroscale model of the matrix phase. The homogenized response of the macroscale continuum model is fitted with the macroscale hyperelastic model.

Macroscale hyperelastic model

Similar to the microscale hyperelastic model, a strain energy density function (W(**C**)) of Ogden type is used. Additionally, to account for hysteresis and the Mullins effect, we introduce a damage variable (η), such that, $\tilde{U}(\mathbf{C}, \eta) = \eta U(\mathbf{C}) + \gamma(\eta)$, as proposed by Ogden and Roxburgh [29]. The damage variable (η) varies continuously during deformation, according to:

$$\eta = 1 - \frac{1}{r}\mathrm{erf}\left(\frac{\tilde{U}^m - U}{m + \beta\tilde{U}^m}\right) \quad (6)$$

where $\tilde{U}^m$ is the maximum value of $\tilde{U}$ at a material point for a given deformation level, (r, m, β) are material parameters, and erf(.) is the error function. The constants (r, m, β) are calibrated as described in "Calibration and validation" section. The macroscale hyperelastic model is then used as constitutive input for the mycelium matrix phased of the composite.

Calibration and validation

The calibration and validation of the composite RVE model is presented in this section. The model has one calibration component, namely the damage parameters (r, m, β) of Eq. (6). The material model of pure mycelium is calibrated and validated in our previous work [9, 19] based on a separate set of experiments performed with pure mycelium. In the current work, we use the validated mycelium model to derive the constitutive input for the mycelium matrix phase, as discussed in "Material model of mycelium matrix" section. The damage parameters (r, m, β) are calibrated by comparing the composite RVE model predicted stress–strain response with the experimental response. The stress–strain curve of a single compression cycle for the "large" particle set is used for this purpose (blue curve in Fig. 4a). Further, the model is validated by predicting the experimental

stress–strain response for multiple compression cycles (Fig. 5a).

Figure 7a compares the prediction of the composite model with the experimental stress–strain curve under a single compression cycle. The predicted stress–strain curve (solid line) is the average of three realizations, and the variability is less than 1% of the mean response (not shown in Fig. 7a). The stress–strain curve for pure mycelium matrix (dash-dot line) is also shown for comparison. The calibrated damage parameters are $r = 1.01$, $m = 0.0001$ and $\beta = 0.02$; with these parameters, the model curve fits the experimental curve well. The response of the composite model in which the set of damage parameters are calibrated based on the pure hyphae experimental data ($r = 1.01$, $m = 0.005$ and $\beta = 0.1$) is used for the matrix which is also shown in Fig. 7a with dashed line. We note that the loading response of the model is a prediction since the material models of both mycelium and reinforcement phases are completely defined in advance, and the damage model has no effect on the loading response.

It is of interest to observe that the curve corresponding to pure mycelium (dash-dot line in Fig. 7a) and the loading branch of the composite curve overlap for the first $\sim 5\%$ engineering strain ($1 > \lambda > 0.95$), which indicates that the small strain response of the composite is entirely controlled by the matrix. The pure mycelium softens at larger strains due to strain localization, while the composite stiffens due to filler–filler interaction.

In Fig. 7b, the model prediction is validated by comparison with the experimental results in Fig. 5a. The damage parameter set ($r = 1.01$, $m = 0.0001$, $\beta = 0.02$) is used here. The composite model is able to predict the generic behavior of mycelium composite during loading. Some discrepancies are observed during unloading which could be due to the limitations of the present model. The matrix–filler interface is treated as well bonded and continuous in the model, while it is discrete and potentially rather weak in reality. It is also possible that plastic deformation of mycelium network contributes to the hysteresis, and this is not accounted for in the model in the absence of reliable data for the plastic deformation of individual hypha. Further, the model has no viscoelastic component and hence it predicts identical unloading and reloading branches, whereas the composite exhibits viscoelastic relaxation of the mycelium matrix upon unloading. Incorporation of such viscoelastic effects is possible (although no accurate experimental data is available) but is not considered central for the current purposes.

Small strain composite modulus

In this section, we investigate the effect of mycelium density on the small strain modulus of the composite. Figure 8 shows the composite modulus (E_c) normalized by the filler particle modulus (E_f), function of the normalized mycelium matrix modulus (E_m/E_f). The mycelium modulus is controlled by the matrix density (ρ_m). We also plotted analytical Hashin–Shtrikman bounds [30] for comparison. It is observed that the results of mycelium-corn composite model

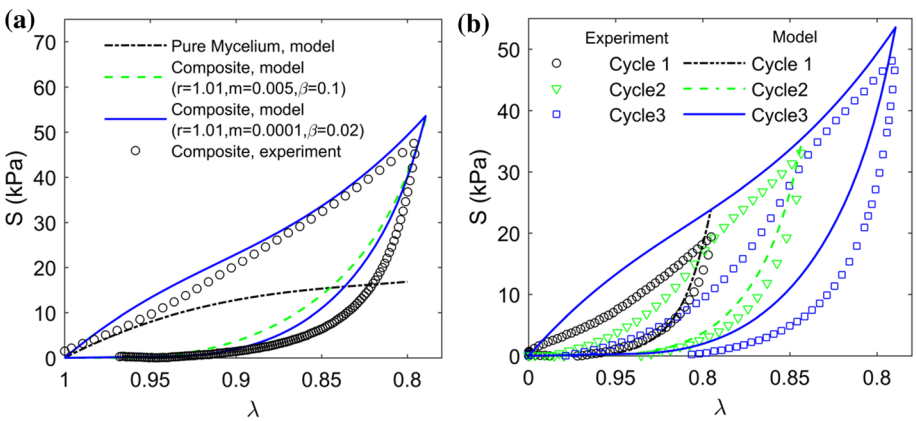

Figure 7 Comparison of model prediction and experimental stress–strain behaviors: **a** single compression cycle (model responses for two damage models (as shown in the legend) and pure mycelium matrix response are shown for comparison) and **b** three successive compression cycles of increasing stretch amplitude.

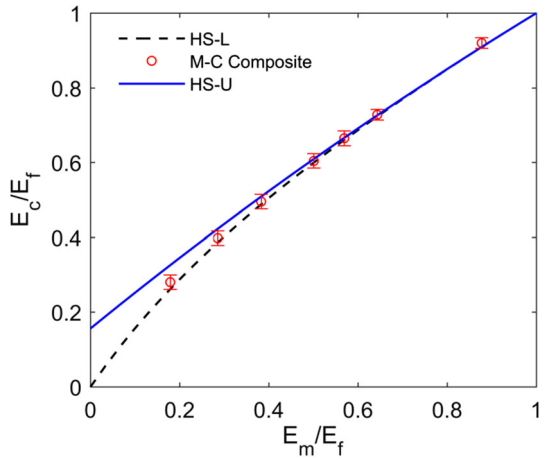

Figure 8 Effect of matrix stiffness (E_m), which in turn is controlled by the matrix density, on composite modulus. The vertical and horizontal axes are normalized by reinforcing particle stiffness (E_f). Hashin–Shtrikman bounds are also shown for comparison.

roughly follow lower bound, indicating the composite modulus is largely dominated by matrix phase.

Effect of particle size

We further analyze the effect of particle aspect ratio and particle size on the mechanical response of the composite. In Fig. 9, model predicted compressive stress–strain responses for various filler aspect ratios (AR = 2, 5 and 8) and sizes (L = 2.5, 5 and 10 mm; d = 0.5, 1, 2 mm) are illustrated for same filler volume fraction (ϕ_f = 0.2). Similar to experiments, we observed that the composite response is independent of the particle size (in the range studied) for a given filler volume fraction. Similar size independence is also reported for other composites such as wood-polymer composites and carbon nanotube reinforced polymers.

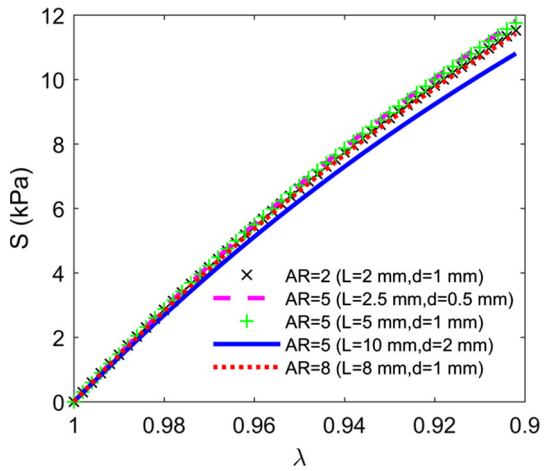

Figure 9 Effect of particle aspect ratio on compressive stress–strain response of mycelium composite.

Conclusions

The mechanical behavior of mycelium composites reinforced with biodegradable agro-waste particles is investigated in this article. The mycelium composite is a multiscale heterogeneous material composed from a fiber network of hyphae which embeds the reinforcing particles. The fillers work both as nutrition for hyphae during growth and as reinforcement during the mechanical function. The behavior of the composite in compression is soft and largely dominated by the mycelium matrix at small strain. At larger strains, rapid stiffening due to the formation of contacts between fillers is observed. The composite exhibits the Mullins effect and hysteresis under cyclic compression—a behavior similar to that of unfilled mycelium. It is also shown that composite properties are largely insensitive to the particle size for given filler volume fraction.

A 3D finite element-based RVE model is presented in which the mycelium network is modeled as homogenized continuum material and reinforcing particles are modeled as linear elastic inclusions. The constitutive behavior of mycelium matrix is obtained from a separate two-scale model which combines a random fiber network-based microscale model with a stochastic continuum model at the macroscale that accounts for mesoscale density fluctuations. The composite RVE model adequately captures the overall behavior, the hysteresis and the Mullins effect. The developed model can be used to predict the material behavior in parametric regimes which are not easily accessible experimentally and for material design. Furthermore, the modeling procedure can be generalized for other soft network-based composites and material systems.

Acknowledgements

This material is based on work supported by the US National Science Foundation (NSF) under Grant CMMI-1362234.

References

[1] Shao Z, Vollrath F (2002) Materials: surprising strength of silkworm silk. Nature 418:741

[2] Gibson LJ (1985) The mechanical behaviour of cancellous bone. J Biomech 18:317–328

[3] Dixon PG, Gibson LJ (2014) The structure and mechanics of Moso bamboo material. J R Soc Interface 11:20140321

[4] Lynch B, Bancelin S, Bonod-Bidaud C, Gueusquin J-B, Ruggiero F, Schanne-Klein M-C, Allain J-M (2017) A novel microstructural interpretation for the biomechanics of mouse skin derived from multiscale characterization. Acta Biomater 50:302–311

[5] Wegst UG, Bai H, Saiz E, Tomsia AP, Ritchie RO (2015) Bioinspired structural materials. Nat Mater 14:23–36

[6] Fricker M, Boddy L, Bebber D (2007) Network organisation of mycelial fungi. In: Howard RJ, Gow NAR (eds) Biology of the fungal cell. Springer, Berlin, pp 309–330

[7] Michalenko G, Hohl H, Rast D (1976) Chemistry and architecture of the mycelial wall of Agaricus bisporus. Microbiology 92:251–262

[8] Howard RJ, Ferrari MA, Roach DH, Money NP (1991) Penetration of hard substrates by a fungus employing enormous turgor pressures. Proc Natl Acad Sci 88:11281–11284

[9] Islam M, Tudryn G, Bucinell R, Schadler L, Picu RC (2017) Morphology and mechanics of fungal mycelium. Sci Rep 7:13070-1–13070-12

[10] Gibson LJ, Ashby MF (1999) Cellular solids: structure and properties. Cambridge University Press, Cambridge

[11] Kim OV, Litvinov RI, Weisel JW, Alber MS (2014) Structural basis for the nonlinear mechanics of fibrin networks under compression. Biomaterials 35:6739–6749

[12] Dorfmann A, Ogden RW (2004) A constitutive model for the Mullins effect with permanent set in particle-reinforced rubber. Int J Solids Struct 41:1855–1878

[13] Mullins L (1969) Softening of rubber by deformation. Rubber Chem Technol 42:339–362

[14] Holt G, Mcintyre G, Flagg D, Bayer E, Wanjura J, Pelletier M (2012) Fungal mycelium and cotton plant materials in the manufacture of biodegradable molded packaging material: evaluation study of select blends of cotton byproducts. J Biobased Mater Bioenergy 6:431–439

[15] Travaglini S, Noble J, Ross P, Dharan C (2013) Mycology matrix composites. In: Proceedings of the American Society for Composites—28th technical conference, State College, PA, pp 1–20

[16] Yang Z, Zhang F, Still B, White M, Amstislavski P (2017) Physical and mechanical properties of fungal mycelium-based biofoam. J Mater Civ Eng 29:04017030-1–04017030-9

[17] Hill R (1963) Elastic properties of reinforced solids: some theoretical principles. J Mech Phys Solids 11:357–372

[18] Kanit T, Forest S, Galliet I, Mounoury V, Jeulin D (2003) Determination of the size of the representative volume element for random composites: statistical and numerical approach. Int J Solids Struct 40:3647–3679

[19] Islam MR, Tudryn G, Bucinell R, Schadler L, Picu RC (2018) Stochastic continuum model for mycelium-based biofoam. Mater Design (submitted)

[20] https://grow.bio/collections/shop/products/hemp-mycelium-material?ref=ecovativeshop (2018)

[21] Islam M, Tudryn GJ, Picu RC (2016) Microstructure modeling of random composites with cylindrical inclusions having high volume fraction and broad aspect ratio distribution. Comput Mater Sci 125:309–318

[22] Evans JW (1993) Random and cooperative sequential adsorption. Rev Mod Phys 65:1281–1329

[23] Version A, 6.13 (2013) Analysis User's Manual. Dassault Systemes Simulia Corp, Providence

[24] Kari S, Berger H, Rodriguez-Ramos R, Gabbert U (2007) Computational evaluation of effective material properties of composites reinforced by randomly distributed spherical particles. Compos Struct 77:223–231

[25] http://www.simmetrix.com/products/SimulationModelingSuite/MeshSim/MeshSim.html

[26] Zhao L, Schaefer D, Xu H, Modi SJ, LaCourse WR, Marten MR (2005) Elastic properties of the cell wall of *Aspergillus nidulans* studied with atomic force microscopy. Biotechnol Prog 21:292–299

[27] Ifuku S, Saimoto H (2012) Chitin nanofibers: preparations, modifications, and applications. Nanoscale 4:3308–3318

[28] Storåkers B (1986) On material representation and constitutive branching in finite compressible elasticity. J Mech Phys Solids 34:125–145

[29] Ogden R, Roxburgh D (1999) A pseudo–elastic model for the Mullins effect in filled rubber. Proc R Soc Lond A Math Phys Eng Sci 455:2861–2877

[30] Hashin Z, Shtrikman S (1963) A variational approach to the theory of the elastic behaviour of multiphase materials. J Mech Phys Solids 11:127–140